Chinese Chemical Letters 31 (2020) 859–864

Contents lists available at ScienceDirect

Chinese Chemical Letters

journal homepage: www.elsevier.com/locate/cclet

Communication

Self-assembled thermosensitive luminescent nanoparticles with peptide-Au conjugates for cellular imaging and drug delivery

Xiaoyuan Zhang[a,b,1], Wei Liu[a,1], Haixia Wang[c,d], Xinne Zhao[a], Zhenfang Zhang[a], Gerd Ulrich Nienhaus[c,d,e,f], Li Shang[g,*], Zhiqiang Su[a,*]

[a] State Key Laboratory of Chemical Resource Engineering, Beijing Key Laboratory of Advanced Functional Polymer Composites, Beijing University of Chemical Technology, Beijing 100029, China
[b] Faculty of Physics and Astronomy, Friedrich Schiller University Jena, Jena 07743, Germany
[c] Institute of Applied Physics, Karlsruhe Institute of Technology (KIT), Karlsruhe 76128, Germany
[d] Institute of Nanotechnology, Karlsruhe Institute of Technology (KIT), Eggenstein-Leopoldshafen 76344, Germany
[e] Institute of Toxicology and Genetics, Karlsruhe Institute of Technology (KIT), Eggenstein-Leopoldshafen 76344, Germany
[f] Department of Physics, University of Illinois at Urbana-Champaign, Urbana, IL 61801, United States
[g] State Key Laboratory of Solidification Processing, Center for Nano Energy Materials, School of Materials Science and Engineering, Northwestern Polytechnical University, Shaanxi Joint Laboratory of Graphene (NPU), Xi'an 710072, China

ARTICLE INFO

Article history:
Received 29 April 2019
Received in revised form 11 June 2019
Accepted 18 June 2019
Available online 19 June 2019

Keywords:
Peptide-Au bioconjugates
PNIPAM nanoparticles
Fluorescence
Drug delivery
Cell imaging

ABSTRACT

A facile and efficient strategy has been developed to fabricate a multifunctional, theranostic anticancer drug delivery platform featuring active targeting, controlled drug release and fluorescence imaging for real-time control of delivery. To this end, thermosensitive poly(*N*-isopropyl acrylamide) (PNIPAM) nanospheres are decorated with peptide-Au cluster conjugates as a smart nanomedicine platform. A sophisticated trifunctional peptide is designed to release the anticancer drug doxorubicin (DOX), target cells and reduce Au^{3+} ions to form luminescent Au clusters. Importantly, the peptide-Au cluster moieties are attached to the PNIPAM nanospheres *via* amide bonds rather than noncovalent interactions, significantly improving their stability in biological medium and drug release efficiency. The *in vitro* experiments showed that DOX was released in an efficient and controlled manner under physiological conditions.

The development of nanoparticles as smart devices for diagnostics and targeted therapeutics has made great progress in recent years [1–4]. However, broad application of nanoparticles in the clinical setting is still fairly limited, often due to inefficacy and poor cell selectivity [5]. Recently, active targeting was developed to overcome the difficulties in release rate and drug distribution control [6,7]. This targeting is typically achieved by functionalizing the drug nanocarriers with biomolecules which can specifically recognize receptors expressed on the cell membranes (*e.g.*, folic acid or arginine-glycine-aspartic acid (RGD) peptide) [8–11]. In contrast to the low efficacy and narrow therapeutic windows of most targeting systems [12,13], active targeting, especially with peptide-based nanocarriers, appears more promising owing to its specific localization capability and clinical safety [14]. Therefore, many efforts have been devoted to peptide-based nanomedicines. Indeed, RGD-based peptides have been frequently integrated into polymeric nanocarrier systems to target therapeutics to integrin-rich solid tumor cells [15–17]. For theranostic peptide nanofiber-graphene quantum dot nanocomposites, it was found that the RGD sequence at the end of short peptides promotes specific uptake by tumor cells, whereas the bright luminescence of quantum dots enabled visualization of the internalized materials inside the tumor cells [18]. This combination of pre-designed RGD-based peptides and fluorescent inorganic nanoparticles, *e.g.*, Au nanoclusters, and graphene quantum dots, suggested a new type of smart drug delivery systems.

In order to develop theranostic nanocarriers that feature active drug targeting, stimulus-responsive drug release and luminescence imaging, we synthesized multifunctional PNIPAM nanospheres decorated with peptide-Au clusters. PNIPAM is a temperature-responsive polymer that allows drug encapsulation within a nanosphere and controlled release of the drug load at

* Corresponding authors.
E-mail addresses: li.shang@nwpu.edu.cn (L. Shang), suzq@mail.buct.edu.cn (Z. Su).
[1] These authors contributed equally to this work.

https://doi.org/10.1016/j.cclet.2019.06.032

elevated temperatures inside the tumor. When the temperature is above the lower critical solution temperature (LCST) of PNIPAM, the chains turn into a contracted, hydrophobic spherical state, resulting in PNIPAM shrinkage and thus controlled drug loading. For peptide decoration, we designed a polypeptide, AAAAAAC-CYRGD consisting of three functional motifs (Fig. 1a). The six alanines of motif 1 (AAAAAA) reduce steric hindrance without affecting the isoelectric point of the polypeptide, and its *N*-terminal amino group can form amide bonds with carboxylate groups on the nanosphere. Motif 2 (CCY) is used to reduce $AuCl_4^-$ ions into clusters using the phenolic group of tyrosine (Y) and to stabilize the clusters via the thiol groups of cysteine (C). Motif 3 (RGD), offers a remarkably high binding affinity to integrin-rich tumor cells [19–21]. Accordingly, this polypeptide plays multiple roles in peptide-Au clusters synthesis, cluster-PNIPAM conjugation and cell targeting. In brief, a design of trifunctionalized peptide, strong fluorescence signal, controlled antitumor drug release, and facile fabrication procedure make this work an attractive candidate for multifunctional anticancer drug delivery platforms, in the fields of controlled release, fluorescence imaging, and targeted therapy.

The peptide-Au clusters were formed by a one-step peptide-mediated biomineralization method. Aqueous solutions of $HAuCl_4$ and NaOH were gently added in sequence to a solution of AAAAAACCYRGD to generate the peptide-Au conjugates. Fig. 1b shows the morphology of peptide-Au clusters imaged by high resolution transmission electron microscopy (HRTEM). These peptide-Au clusters have low size dispersion, and their average diameters were measured to be 1.80 ± 0.45 nm with fine crystalline structure. This result is in good agreement with that obtained from the analysis of atomic force microscopy (AFM) height images (Fig. S1 in Supporting information). The crystalline interplanar distance is 0.21 nm, corresponding to the (111) plane of Au(0) [22,23]. The cluster size is in the range of the Fermi wavelength of the conduction electrons, which governs the optical properties of the nanoclusters [24]. Accordingly, the free electrons are spatially confined in the Au clusters and their electronic transitions yield interesting optical properties, notably luminescence, making Au clusters attractive in diagnostic and therapeutic applications [25].

The absorption spectra of peptide-Au clusters (Figs. 1c and d) show featureless absorption in the visible range and a weak band of the peptide ligands near 280 nm. The pronounced excitation and emission peaks of peptide-Au clusters are observed at 500 nm and 670 nm, respectively. The near-infrared emission band is attractive for thick tissue imaging because of the reduced scattering at long wavelength and the resulting enhanced tissue penetration [23,26–28]. As shown in Fig. 1d, the emission spectrum remains essentially unchanged when the excitation wavelength is varied between 410 nm and 530 nm, as expected from Kasha's rule and confirming that the observed photoemission is indeed from the Au clusters. Fig. 1e shows photographs of peptide-Au clusters luminescence under 365 nm but not under visible light excitation.

PNIPAM nanospheres afford efficient loading and controlled release of anticancer drugs. In this case, PNIPAM–COOH (Fig. 2a), a temperature-responsive polymer with a carboxylic acid-ended group, was prepared by free radical polymerization between NIPAM monomers and β-mercaptopropionic acid (MPA) by using azobisisobutyronitrile (AIBN) as the initiator [29,30]. Representative TEM images of the formed PNIPAM–COOH nanospheres are shown in Fig. S2 (Supporting information). Their diameters ranged from 120 nm to 300 nm, which is a suitable size for drug nanocarriers.

Using 1-ethyl-3-(3-dimethylaminopropyl) carbodiimide (EDC) and *N*-hydroxysuccinimide (NHS) as coupling agents, peptide-Au clusters were covalently bound to the surface of PNIPAM–COOH nanospheres *via* amide bonds (Fig. 2b), resulting in compact,

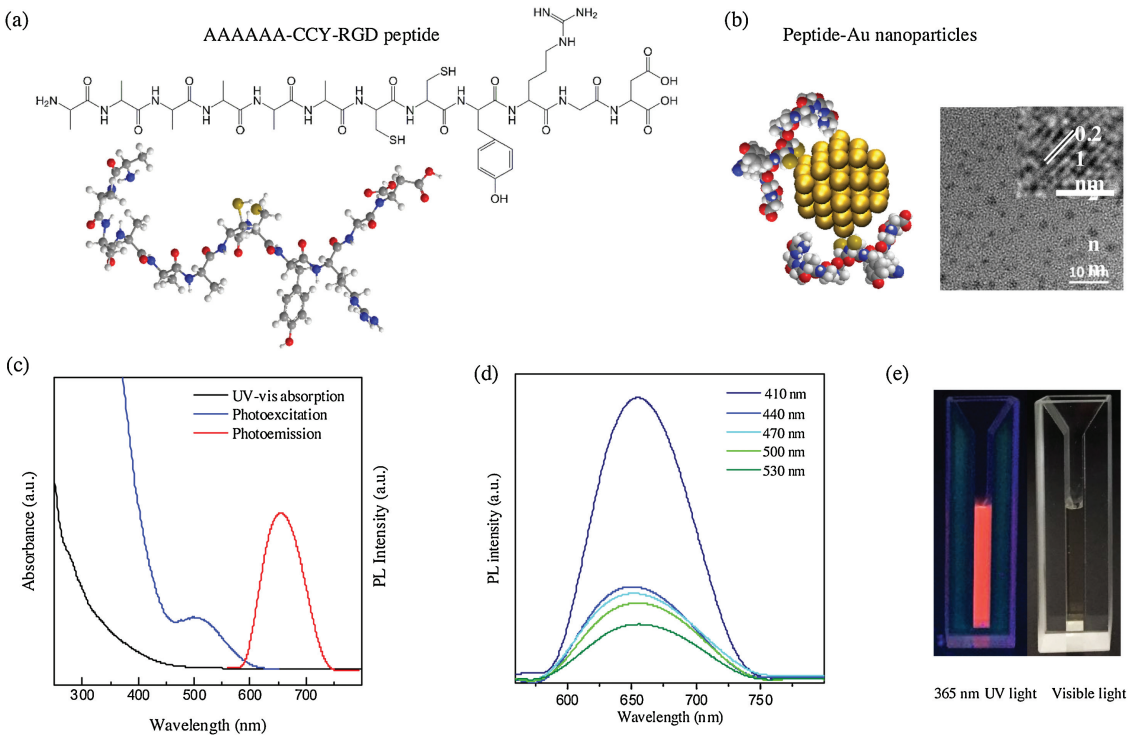

Fig. 1. (a) The chemical structure and a ball-and-stick depiction of the trifunctional peptide. (b) Van-der-Waals model and HRTEM image of peptide-Au cluster. (inset: close-up of a selected Au cluster, showing its crystalline structure.) (c) UV–vis absorption (black line), excitation (blue line, $\lambda_{em} = 670$ nm) and emission (red line, $\lambda_{ex} = 410$ nm) spectra of peptide-Au clusters. (d) Emission spectra of peptide-Au clusters with different excitation wavelength ranging from 410 nm to 530 nm. (e) Photographs of peptide-Au clusters under 365 nm UV (left) and visible (right) light illumination.

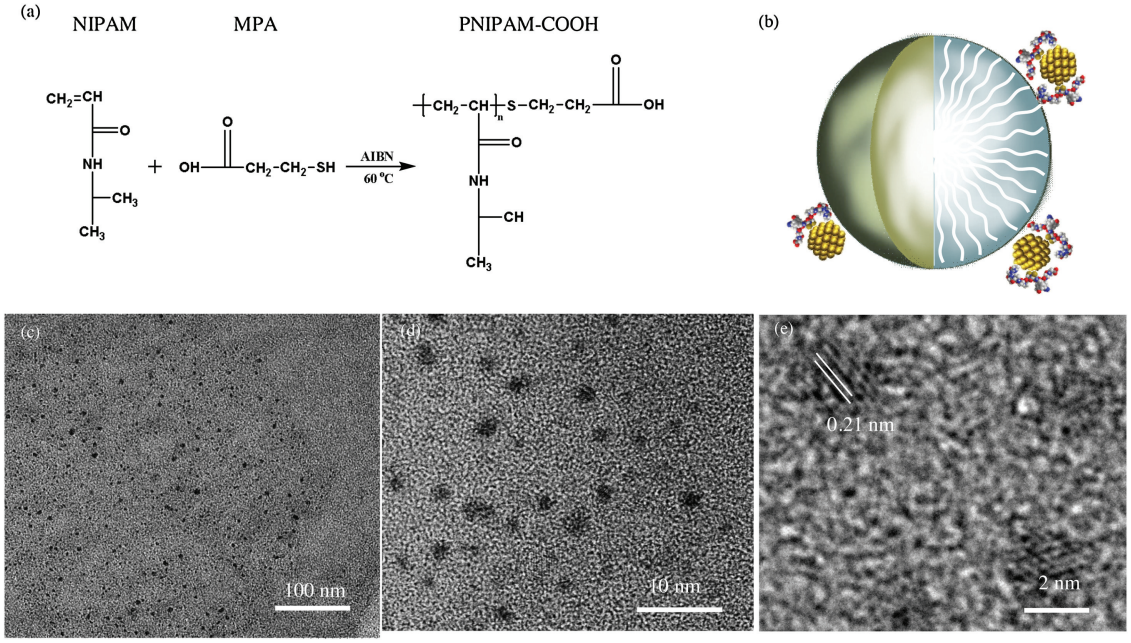

Fig. 2. (a) Synthesis of PNIPAM–COOH. (b) Schematic drawing of PNIPAM-peptide-Au nanospheres. Representative (c) TEM and (d) HRTEM image of peptide-Au clusters on PNIPAM-Au-peptide nanospheres. (e) Close-up of selected peptide-Au clusters, revealing their crystalline structure.

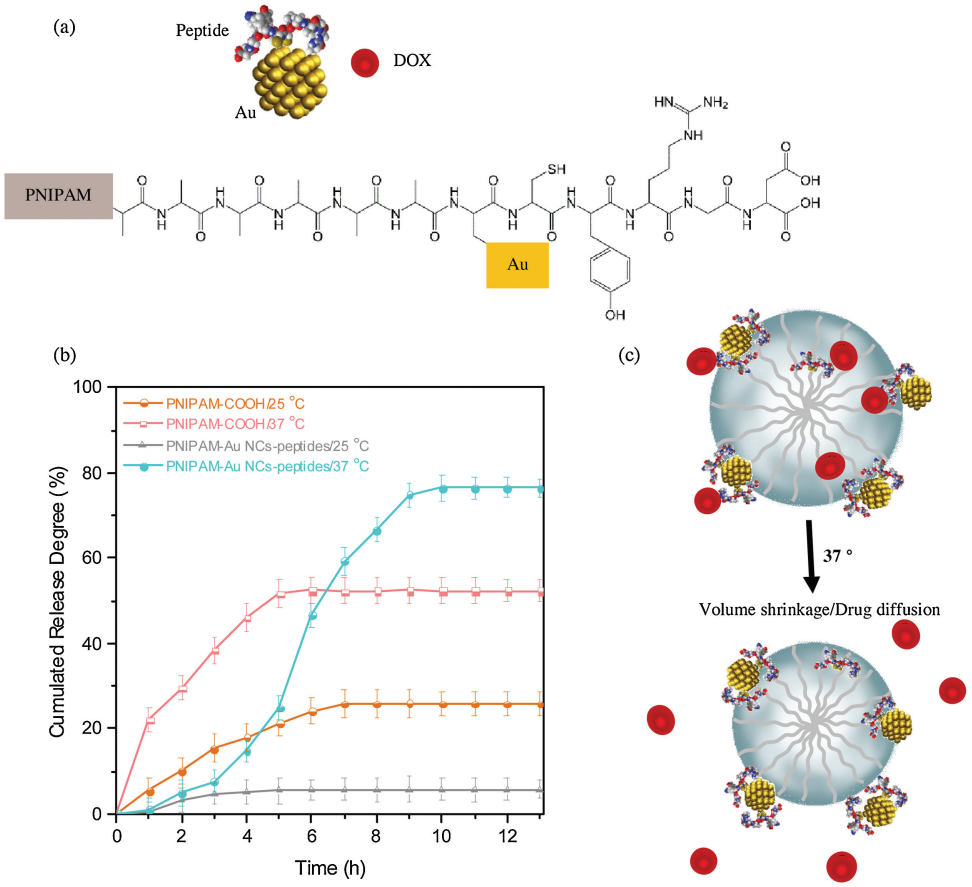

Fig. 3. (a) Synthetic route of PNIPAM-Au-peptide nanospheres and its interaction with DOX. (b) The drug release kinetics of DOX from PNIPAM–COOH and PNIPAM-Au-peptide nanospheres at 37 °C and 25 °C. (c) Schematically drawing of the proposed release mechanisms.

peptide-Au cluster-decorated nanospheres. The LCST of PNIPAM-Au-peptide was measured to be 33 °C, indicating that the Au-peptide modification preserved the thermosensitivity of the nanospheres (Fig. S5 in Supporting information). Covalent bond formation also improved the stability of PNIPAM-peptide-Au nanospheres.

The TEM images in Figs. 2c–e show many small particles surrounding a big circle, clearly revealing peptide-Au clusters on the PNIPAM–COOH nanosphere surfaces and confirming the successful conjugation of peptide-Au clusters to PNIPAM–COOH nanospheres. As expected, the sizes of PNIPAM-peptide-Au nanospheres remained essentially unchanged compared with PNIPAM–COOH nanospheres. The ordered lattice planes of the peptide-Au clusters in the HRTEM micrograph further confirmed the presence of crystalline peptide-Au clusters in the composite nanospheres (Fig. 2e). Their spacing was about 0.21 nm, corresponding to (111) planes of Au(0). Thus, the presence of PNIPAM–COOH did not influence the crystal structure and particle size of the peptide-Au clusters on the nanospheres.

PNIPAM-peptide-Au nanospheres emit intense red light under excitation at 365 nm. As shown in Fig. S2f (Supporting information), the luminescence peak of peptide-Au clusters shifted slightly after conjugating with PNIPAM–COOH, which is likely due to the influence of the polymer chain structure. Further characterization by zeta potential and XPS measurements also confirmed the successful formation of nanospheres (Figs. S3 and S4 in Supporting information).

The temperature sensitivity of PNIPAM is due to the presence of hydrophilic amide groups and hydrophobic isopropyl groups. The LCST of PNIPAM (*ca.* 32 °C) is close to human body temperature, which is of critical importance for the construction of a drug release system [31]. At room temperature, the PNIPAM–COOH solution is a colorless, transparent liquid. When the temperature is raised to 37 °C, the solution gradually turns into an opaque milky liquid. This is mainly due to the phase transition of PNIPAM–COOH caused by hydrogen bond changes [32,33]. Our results showed that the LCST of the PNIPAM-peptide-Au is about 33 °C, suggesting the potential utility of these nanospheres as thermosensitive drug

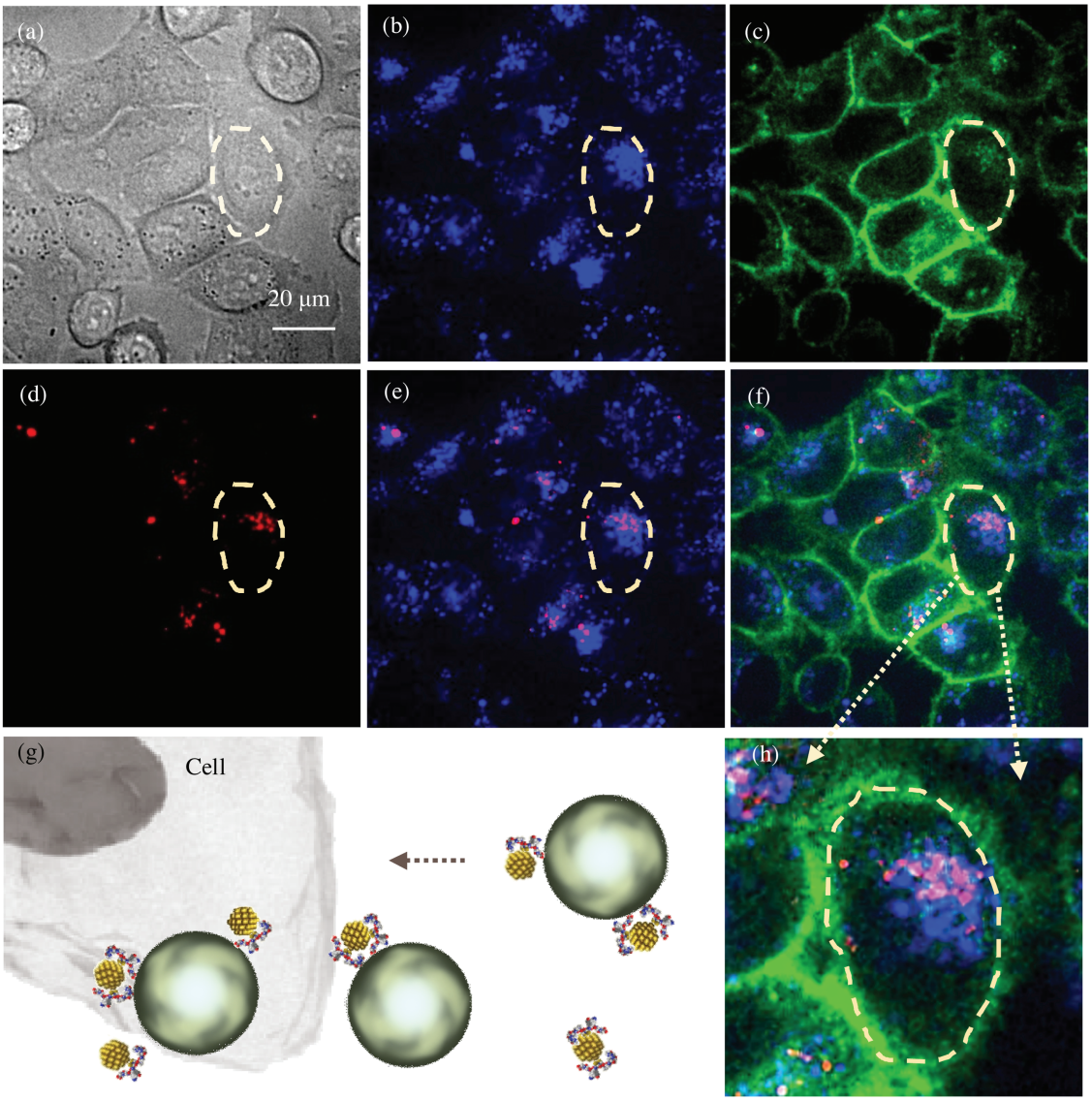

Fig. 4. (a–f) Spinning disk confocal fluorescence images of cultured HeLa cells in DMEM after incubation with PNIPAM-Au-peptide nanospheres for 2 h (gray, bright field; red, PNIPAM-Au-peptide; blue, lysosomal marker; purple, colocalization of red and blue; green, membrane). (g) Schematically drawing of proposed model for nanosphere-cell interactions. (h) The magnified image of nanoclusters-loaded cell from (f).

nanocarriers (Fig. S5 in Supporting information). When the temperature is lower than the LCST, hydrogen bonds are formed between the amide groups on the PNIPAM−COOH and water molecules, thus the PNIPAM−COOH chains exhibit a stretched and hydrophilic coil state. However, when the temperature is above the LCST, the formed hydrogen bonds break and the PNIPAM−COOH chains turn into a contracted, hydrophobic spherical state, leading to compaction and shrinkage of PNIPAM−COOH. In the nanosphere formation process, most of the peptide-Au clusters are decorated on the PNIPAM−COOH surfaces as shell. Note that the distribution and size of the nanoclusters did not influence the thermal sensitivity of the PNIPAM−COOH nanospheres.

DOX, a widely used antitumor drug [34], was chosen to evaluate the drug delivery potential of our system into cancer cells. The initial drug loading content was obtained using the following equation, loading content (w/w) = (weight of loaded drug/weight of added nanospheres) × 100%. The value was calculated to be 12.3% ± 0.4% for PNIPAM-Au-peptide nanospheres. The initial loading content of DOX in PNIPAM−COOH nanospheres was comparable to that of PNIPAM-Au-peptide nanospheres. Regarding the release of DOX at different temperatures (below or above the LCST), the thermal response of PNIPAM-peptide-Au nanospheres plays a vital role (Fig. 3a). Release curves of DOX from drug-loaded PNIPAM−COOH nanospheres and PNIPAM-peptide-Au nanospheres at 25 °C (below LCST) and 37 °C (above LCST) are shown in Fig. 3b. It was reported that, DOX molecules possess an adsorption peak at 480 nm [35]. Therefore, the amount of released DOX can be measured *via* the UV absorbance at 480 nm. Meanwhile, we noted that one can also confirm the successful release of DOX molecules by well-established techniques such as high-performance liquid chromatography-mass spectrometry (HPLC-MS) [36,37].

The cumulative release degree, f, of DOX at a particular time, t, is given by $f(t) = W(t)/W_0$, where $W(t)$ is the mass of DOX released at time t and W_0 is the total mass of loaded DOX. For both nanospheres, the fraction released was markedly higher at 37 °C than that at 25 °C. DOX release from PNIPAM-peptide-Au nanospheres showed a pronounced temperature effect, reaching 6% in ∼4 h at 25 °C and 77% in ∼10 h at 37 °C. A change between 36 °C and 40 °C would be interesting for targeted delivery because of the higher temperature in solid tumors [38]. By contrast, DOX release from PNIPAM−COOH nanospheres saturated at 26% at 25 °C and at 52% at 37 °C within ∼6 h at both temperatures. Thus, PNIPAM-peptide-Au nanospheres displayed a much larger thermal response of DOX release than PNIPAM−COOH nanospheres. When the temperature is 37 °C (above the LCST), the PNIPAM chains transform from a stretched and hydrophilic coil state to a contracted and hydrophobic spherical state, leading to shrinkage of PNIPAM-Au-peptide nanospheres and release of drug (Fig. 3c). Moreover, it is well known that DOX is positively charged [39,40], resulting in strong electrostatic interactions with negatively charged PNIPAM-Au-peptide nanospheres. We speculate that this result can be attributed to two factors. The main reason should be the elimination of the blocking DOX in the interspace, which is formed between peptide-Au clusters on the PNIPAM−COOH nanosphere surfaces. Secondly, the formed amide bonds between shell and core facilitate the squeeze of the peptide-Au clusters against the PNIPAM−COOH nanospheres, leading to a tighter nanoparticles and more effective drug release manner at 37 °C.

Next, we explored the potential application of PNIPAM-peptide-Au nanospheres for cellular imaging. HeLa cells were cultured in DMEM containing PNIPAM-peptide-Au nanospheres. The images in Fig. 4, taken with a spinning disk confocal microscope, of HeLa cells after incubation with PNIPAM-peptide-Au nanospheres show luminescence from PNIPAM-peptide-Au nanospheres (in red), fluorescence from a lysosomal marker (LysoTracker Blue) in blue, and fluorescence from the plasma membrane (CellMaskTM Green) in green. Notably, bright red emission from PNIPAM-peptide-Au nanospheres is mainly co-localized with lysosomes (Figs. 4d–f), showing that PNIPAM-peptide-Au are efficiently internalized into HeLa cells *via* the endosomal pathway and end up in lysosomes. Moreover, the presence of the RGD sequence in our peptide-Au clusters can promote the cellular internalization of PNIPAM-peptide-Au nanospheres (Fig. 4g). In addition, the cytotoxicity of these nanospheres was evaluated by using an MTT assay method with HeLa cells. As shown in Fig. S6 (Supporting information), for PNIPAM-peptide-Au nanosphere concentration in the range of 0.04–2.5 μmol/L, cell survival was higher than of the controlgroup, which indicates low cytotoxicity of PNIPAM-peptide-Au nanospheres.

In summary, we have reported a novel type of hybrid nanostructure, peptide-Au nanocluster-decorated polymer nanospheres, which is capable of controlled drug release and cell imaging. The multi-motif design of the peptide sequence enables the construction of multifunctional nanomedicine platform with distinct advantages, including facile materials fabrication, thermosensitivity, low cytotoxicity, and near-IR bio-imaging capability. We note that the current strategy is rather flexible and can be easily extended to fabricate other nanosystems by employing custom-designed peptides or nanoprobes. While we have shown promising cellular level results in the present study, *in vivo* investigations will be performed to bring this nanomedical platform closer to a concrete biomedical application.

Acknowledgments

The authors gratefully acknowledge financial support from the National Natural Science Foundation of China (NSFC, Nos. 51573013, 51873016). X. Zhang gives thanks to the China Scholarship Council (CSC) for a Ph.D scholarship. L. Shang acknowledges support from the Shaanxi Natural Science Foundation (No. 2018JM2004) and NSFC (No. 21705129). G.U. Nienhaus was funded by the Helmholtz association, program Science and Technology of Nanosystems (STN).

Appendix A. Supplementary data

Supplementary material related to this article can be found, in the online version, at doi:https://doi.org/10.1016/j.cclet.2019.06.032.

References

[1] G.F. Luo, W.H. Chen, S. Hong, et al., Adv. Funct. Mater. 27 (2017) 1702122–1702134.
[2] H.W. Sung, Z. Liu, Adv. Healthc. Mater. 3 (2014) 1130–1132.
[3] S. Bazban-Shotorbani, M.M. Hasani-Sadrabadi, A. Karkhaneh, et al., J. Control. Release 253 (2017) 46–63.
[4] X. Zhou, Y. Hao, L. Yuan, et al., Chin. Chem. Lett. 29 (2018) 1713–1724.
[5] S. Nazir, T. Hussain, A. Ayub, U. Rashid, A. MacRobert, J. Nanomedicine. 10 (2014) 19–34.
[6] O.C. Farokhzad, R. Langer, ACS Nano 3 (2009) 16–20.
[7] Q. Liu, H. Wang, G. Li, et al., Chin. Chem. Lett. 30 (2019) 485–488.
[8] H. Meng, Y. Zou, P. Zhong, et al., Macromol. Biosci. 17 (2017) 1600518–1600525.
[9] H. Wang, J. Li, X. Zhang, et al., RSC Adv. 3 (2013) 9304–9310.
[10] J. Boucard, C. Linot, T. Blondy, et al., Small 14 (2018) 1802307.
[11] E. Teston, T. Maldiney, I. Marangon, et al., Small 14 (2018) 1800020.
[12] X. Zeng, G. Liu, W. Tao, et al., Adv. Funct. Mater. 27 (2017) 1605985.
[13] X. Wang, M. Zeng, Y.H. Yu, et al., ACS Appl. Mater. Interfaces 9 (2017) 7852–7858.
[14] Y. Li, W. Zhang, L. Zhang, et al., Adv. Mater. Interfaces 4 (2017) 1600895.
[15] G. Wei, Z. Su, N.P. Reynolds, et al., Chem. Soc. Rev. 46 (2017) 4661–4708.
[16] G.B. Qi, Y.J. Gao, L. Wang, H. Wang, Adv. Mater. 30 (2018) 1703444.
[17] W. Zhang, X. Yu, Y. Li, et al., Prog. Polym. Sci. 80 (2017) 94–124.
[18] Z. Su, H. Shen, H. Wang, et al., Adv. Funct. Mater. 25 (2015) 5472–5478.
[19] Y. Wang, Y. Cui, Y. Zhao, et al., Chem. Commun. (Camb.) 48 (2012) 871–873.
[20] Y. Yi, H.J. Kim, P. Mi, et al., J. Control. Release 244 (2016) 247–256.
[21] W. Zhang, D. Lin, H. Wang, et al., Bioconjugate Chem. 28 (2017) 2224–2229.
[22] M. Chen, D. Wang, X. Liu, RSC Adv. 6 (2016) 9549–9553.

[23] T. Fujigaya, C. Kim, Y. Hamasaki, N. Nakashima, Sci. Rep. 6 (2016) 21314–21323.
[24] J. Xie, Y. Zheng, J.Y. Ying, J. Am. Chem. Soc. 131 (2009) 888–889.
[25] Y. Negishi, N.K. Chaki, Y. Shichibu, R.L. Whetten, T. Tsukuda, J. Am. Chem. Soc. 129 (2007) 11322–11323.
[26] J. Zheng, P.R. Nicovich, R.M. Dickson, Annu. Rev. Phys. Chem. 58 (2007) 409–431.
[27] J. Zheng, C.W. Zhang, R.M. Dickson, Phys. Rev. Lett. 93 (2004) 177402.
[28] L. Shang, L. Yang, F. Stockmar, et al., Nanoscale 4 (2012) 4155–4160.
[29] J. Tang, X. Cui, T.G. Caranasos, et al., ACS Nano 11 (2017) 9738–9749.
[30] C.L. Zhang, F.H. Cao, J.L. Wang, et al., ACS Appl. Mater. Interfaces 9 (2017) 24857–24863.
[31] R. Contreras-Cáceres, A. Sánchez-Iglesias, M. Karg, et al., Adv. Mater. 20 (2008) 1666–1670.
[32] S. Murphy, S. Jaber, C. Ritchie, M. Karg, P. Mulvaney, Langmuir 32 (2016) 12497–12503.
[33] J. Malinge, F. Mousseau, D. Zanchi, et al., J. Colloid Interface Sci. 461 (2016) 50–55.
[34] J.H. Park, L. Gu, G. von Maltzahn, et al., Nat. Mater. 8 (2009) 331–336.
[35] N. Husain, R.A. Agbaria, I.M. Warner, J. Phys. Chem. 97 (1993) 10857–10861.
[36] R.J. Amir, M. Popkov, R.A. Lerner, C.F. Barbas III, D. Shabat, Angew. Chem. Int. Ed. 44 (2005) 4378–4381.
[37] L. Gu, J.H. Park, K.H. Duong, E. Ruoslahti, M.J. Sailor, Small 6 (2010) 2546–2552.
[38] H.C. Huang, K. Rege, J.J. Heys, ACS Nano 4 (2010) 2892–2900.
[39] W.F. Ma, K.Y. Wu, J. Tang, et al., J. Mater. Chem. 22 (2012) 15206–15214.
[40] S. Guo, X. Xiao, X. Wang, et al., Biomaterials Sci. 7 (2019) 1919–1932.